



Research Article

ISSN : 0975-7384  
CODEN(USA) : JCPRC5

## Synthesis, spectral, computational and biological study of Co(II), Ni(II), Cu(II) and Zn(II) complexes with azo dye derived from 4,4'-diaminodiphenylsulphone and 5-sulphosalicylic acid

S. N. Chaulia

P. G. Department of Chemistry, G. M. (Autonomous) College, Sambalpur, Odisha, India

### ABSTRACT

Metal complexes of Co(II), Ni(II), Cu(II) and Zn(II) with azo dye 4,4'-bis(2'-hydroxy-3'-carboxy-5'-sulphophenylazo)diphenylsulphone derived from 4,4'-diaminodiphenylsulphone and 5-sulphosalicylic acid have been synthesised. The ligand and complexes have been characterised by analytical, conductance, spectral, magnetic susceptibility, thermal, X-ray diffraction pattern, surface morphological and computational study. The ligand LH<sub>2</sub> is a hexadentate chelating ligand as indicated from the physicochemical studies and spectral data. The spectral and analytical data also reveal distorted octahedral geometry for the Co(II), Ni(II) and Cu(II) complexes and distorted tetrahedral geometry for the Zn(II) complex. The thermal study depicts thermal stability of the complexes and the XRD (powder pattern) study of the Cu(II) complex indicates cubical crystal system. The synthesised compounds can also act photoactive material as suggested from the fluorescence studies and the SEM image provides the surface morphology of the Zn(II) complex. The biological study of the azo compounds indicates the metal compounds are more active than the ligand against the pathogenic bacteria and metal complexes have more DNA binding activity than the ligand. The computational study of the ligand and its metal complexes have been made through DFT theory to look in to their reactivity's and geometrical parameters.

**Keywords:** chelating ligand, fluorescence studies, SEM image, DNA binding

### INTRODUCTION

The study of azo dyes and their metal complexes has been of much interest in recent years due to their application in various fields such as textile dyes[1], acid-base and red ox indicators[2] and metalochromic reagents[3], biomedical studies and potential drugs[4,5] and high technology area such as laser and electro-optical devices[6,7]. Azo compounds are also involved in a number of biological reactions like antibacterial, antifungal, DNA binding activity, protein synthesis [8]. The Azo compounds derived from 4,4'-diaminodiphenylsulphone and its metal complexes is reported to have biological activity[9] that prompted me to prepare azodye from 4,4'-diaminodiphenylsulphone and 5-sulphosalicylic acid, its metal complexes, to characterise them by various physico-chemical and spectra techniques and to evaluate their biological activities.

### EXPERIMENTAL SECTION

All chemicals used are analytical grade procured from High-media and doubly distilled water was used in all experiments. Elemental analysis of the ligand and complexes is carried out by Perkin –Elmer elemental analyser, cobalt, nickel, copper contents is determined by Perkin –Elmer2380 atomic absorption spectroscopy and chloride contents is estimated by standard procedure, Systronic conductivity bridge 30 is used to measure molar conductance of the complexes, Magnetic susceptibility of the complexes is measured by Guoy<sup>s</sup> balance using Hg[Co(NCS)<sub>4</sub>] as a calibrant at room temperature and diamagnetic correction have been made by pascal's constants, IR spectra of the

ligand and metal complexes are recorded on a using KBr pellets by perkin elmer FT- IR spectrometer within the range 4000- 450  $\text{cm}^{-1}$ , UV-Visible spectra of the complexes are collected using a THERMO SPECTRONIC 6 HEXIOS  $\alpha$  and fluorescence spectra are recorded in a Fluorescence spectrometer,  $^1\text{H}$  NMR spectra of the ligand and the Zn(II) complex are obtained from Bruker AV III 500 MHZ FT NMR spectrometer using TMS as reference, ESR spectrum of the Cu(II) complex is recorded on JES-FA 200 ESR spectrometer , mass spectra of the ligand and its complexes are recorded through JEOL GC Mate GC-MS Mass Spectrometer, thermal study of the metal complex is done by NETZSCH STA 449 F3 JUPITOR, SEM image of the complexes are taken in JES FA 200, the XRD powder pattern of the Cu(II) complex is collected using a Philips X'Pert Pro diffractometer.

In order to get the better picture about reactivity and geometrical parameters, computational study of the ligand and the metal complexes are performed by Gaussian 03 software package[10].The molecular geometry of the ligand and its complex are fully optimised using B3LYP[11] level of theory along with 6-31G(d,p) basis set. The B3LYP provides better results than the Hartree-Fock method and reproduce better geometrical parameters comparable to the experimental values.

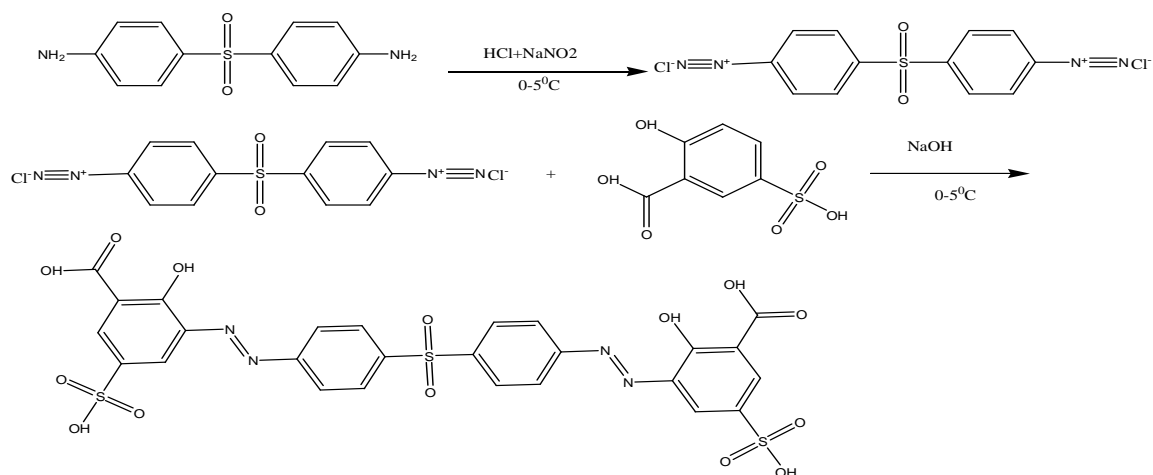
The DNA binding study of the azo compounds is made by Gel electrophoresis[12] method. 10  $\mu\text{L}$  of the metal complexes are taken along with 15  $\mu\text{L}$  of CT DNA solution dissolved in Tris-EDTA in centrifuge tubes. The tubes are incubated at 37°C for 1 hour. After incubation, the tubes containing solution are kept in a refrigerator at 0°C for few minutes, 5  $\mu\text{L}$  gel loading buffer with tracking dye (0.25% bromo phenol) is taken in the tubes for electrophoresis. The electrophoresis is continued under constant voltage (50 V) and photographed under UV illumination.

Hydrodynamic volume change[13] is observed by Ostwald Viscometer immersed in a thermostatic bath maintained at 37°C . A digital stopwatch is used to measure the flow time, mixing of complexes under investigation with CT-DNA is carried out by bubbling nitrogen. Data are presented by plotting a graph indicating  $(\eta/\eta_0)^{1/3}$  versus  $[\text{complex}]/[\text{DNA}]$  where  $\eta$  is the viscosity of DNA in presence of complexes and  $\eta_0$  represents the viscosity of DNA alone. Viscosity values are collected by following the equation  $\eta = t - t_0$  where  $t$  is the flow time of the DNA containing solutions and  $t_0$  is the flow time of DNA alone.

The antibacterial activity of the ligand and its metal complexes is studied in vitro by the cup-plate method[14] against the *Escherichia coli* (MTCC-40)and *Staphylococcus aureus* (MTCC-87)using agar nutrient as the medium by the cup plate method[14]. The investigated ligand and its complexes are dissolved in DMF. The sterilised agar plates are swabbed with the bacteria culture and filled with test solutions, then incubated at 37 °C for 24 hours. The activity is evaluated by measuring the zone of inhibition with respect to the standard drug Tetracycline.

#### Synthesis of the ligand

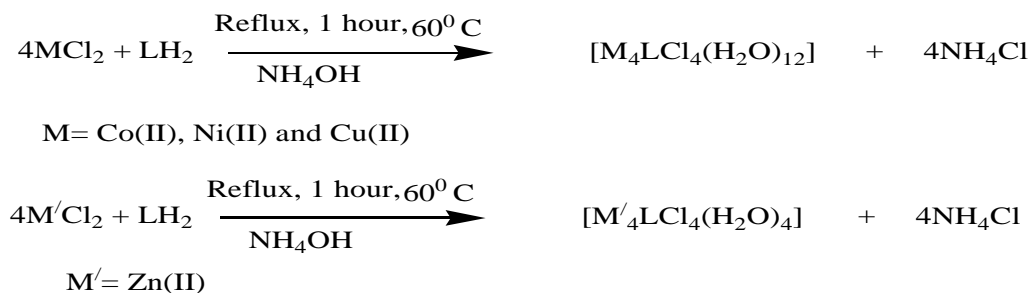
The ligand LH<sub>2</sub> was prepared by the coupling reaction between the diazonium salt solution and the alkaline solution of 5-sulpho salicylic acid. The diazonium salt solution was made by dissolving 4, 4'-diaminodiphenyl sulphone(0.01 mol,1.98 g) in hydrochloric acid at 0-5°C, solution and sodium nitrite . This solution was then added to the ice cooled alkaline solution of 5-sulpho salicylic acid(0.02mol,4.36 g) with stirring. The red coloured azo compound was collected by vacuum filtration, recrystallised from ethanol and dried in vacuum[Reaction scheme-1].



#### Reaction Scheme-1

#### Synthesis of metal complexes

The metal chlorides in ethanol were mixed with the DMF solution of the ligand in 4:1 molar ratio separately and the resulting solutions were refluxed for one hour at 60°C. The refluxed solutions were allowed to cool and concentrated Ammonia solution was added drop by drop till the formation of precipitates. The precipitates of azo metal complexes [Fig-1, Fig-2] were collected by filtration, washed with ethanol and dried in vacuum [Reaction Scheme-2].



Reaction Scheme-2

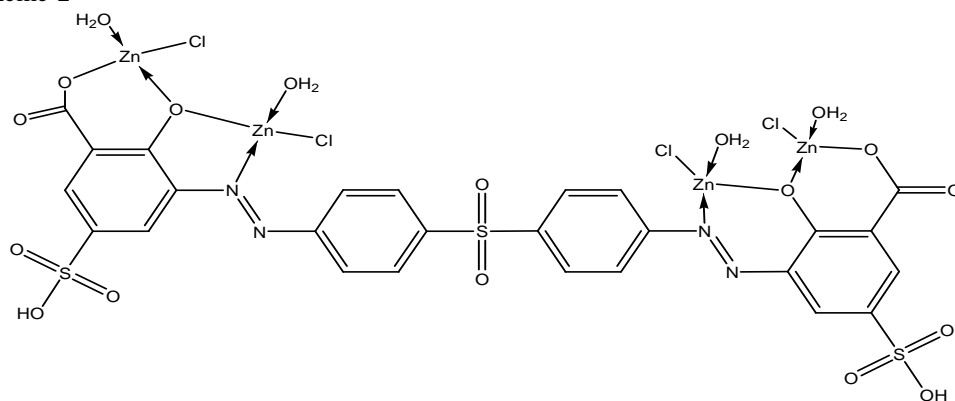


Fig-1. Figure of Zn(II) complex

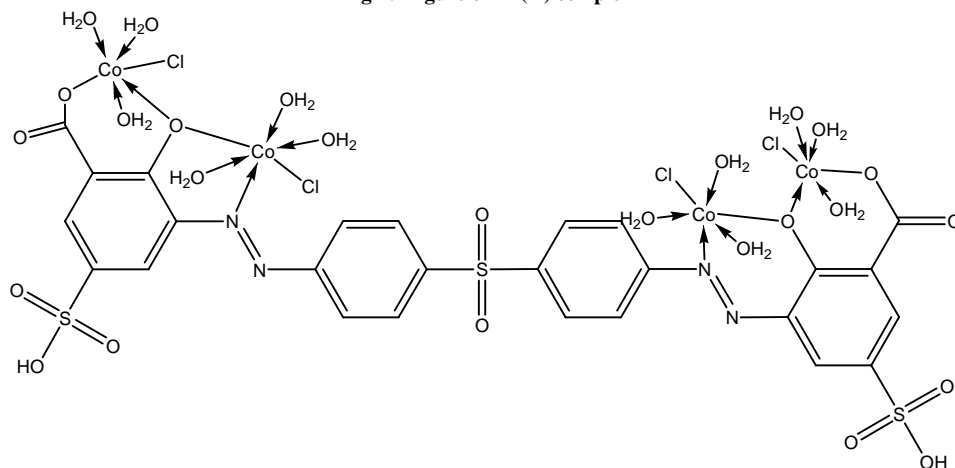


Fig-2. Figure of Co(II) complex

## RESULTS AND DISCUSSION

### Elemental analysis and conductance measurement

The analytical and physical properties of the Azo dye and its complexes are presented in Table-1 which are in good agreement with calculated values. The molar conductance of the complexes with  $1 \times 10^{-3}$  M DMSO solution are found to be in the range of  $9.1\text{--}12.5 \text{ ohm}^{-1}\text{cm}^2\text{mol}^{-1}$  indicating non-electrolytic nature[15]. All compounds are insoluble in ethanol, methanol, acetone, ether, chloroform but soluble in DMF and DMSO.

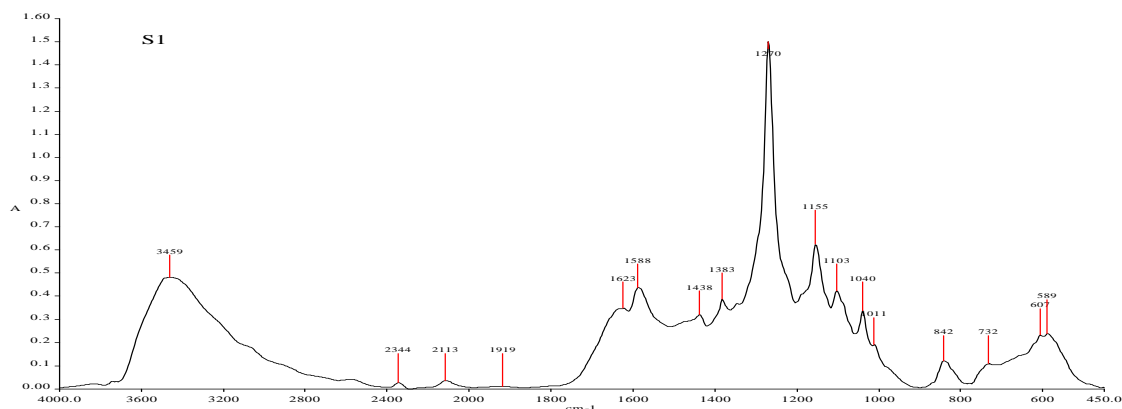
Table-1 Analytical data

Compound	Colour	Yield(%)	M.P (°C)	% Found(calcd)					
				M	C	H	N	Cl	S
1	purple	76	68	-	44.05 (44.19)	2.12 (2.57)	7.65 (7.93)	-	13.23 (13.61)
2	red	58	>300	17.85 (18.18)	24.01 (24.09)	2.25 (2.95)	4.01 (4.32)	10.63 (10.94)	7.12 (7.42)
3	Light red	54	>300	17.78 (8.1201)	24.06 (24.11)	2.73 (2.96)	4.06 (4.33)	10.59 (10.95)	7.19 (7.43)
4	green	62	>300	18.97 (19.19)	23.26 (23.75)	2.82 (2.91)	4.03 (4.26)	10.55 (10.790)	7.08 (7.32)
5	Light pink	65	>300	21.89 (22.20)	26.13 (26.51)	1.57 (1.88)	4.33 (4.76)	11.92 (12.04)	8.05 (8.17)

### 1.LH<sub>2</sub>, 2.[Co<sub>4</sub>LCl<sub>4</sub>(H<sub>2</sub>O)<sub>12</sub>], 3.[Ni<sub>4</sub>LCl<sub>4</sub>(H<sub>2</sub>O)<sub>12</sub>], 4.[Cu<sub>4</sub>LCl<sub>4</sub>(H<sub>2</sub>O)<sub>12</sub>], [Zn<sub>4</sub>LCl<sub>4</sub>(H<sub>2</sub>O)<sub>4</sub>]

#### IR spectra and mode of bonding

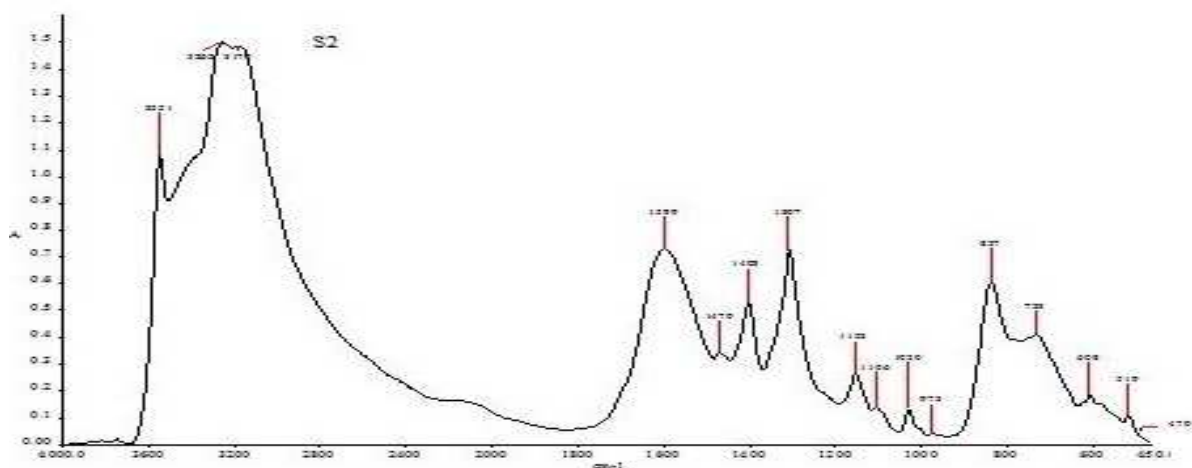
The IR spectrum (Graph-1) of the ligand was compared with the spectra of metal complexes (Graph-2, Table-2) in order to examine the mode of bonding between ligand and complexes. The IR spectrum of the ligand shows a broad band at 3459 cm<sup>-1</sup> which is missing from the spectra of the metal complexes that indicates deprotonation of phenolic(-OH) and bonding metal atom with oxygen atom of the -OH group. The C-O frequency vibration band observed at 1438 cm<sup>-1</sup> in ligand is shifted to ~1406 cm<sup>-1</sup> in complexes confirming[16] bonding of metal with oxygen atom of -OH group. Two bands appears at 1383 and 1625 cm<sup>-1</sup> corresponding to  $\nu_{\text{sym}}$  and  $\nu_{\text{asym}}$  respectively in the spectrum of the ligand which are observed at ~1307 cm<sup>-1</sup> and ~1599 cm<sup>-1</sup> due to  $\nu_{\text{sym}}$  and  $\nu_{\text{asym}}$  that indicates monodentate nature of carboxylate group[17] and bonding of carboxylic oxygen with metal atoms. A band appears at 1588cm<sup>-1</sup> corresponds to -N=N- group in the ligand is shifted to ~ 1470 cm<sup>-1</sup> that suggests bonding of azo nitrogen with the metal atom[18]. The presence of coordinated water in metal complexes is confirmed[19] by the stretching band at ~3262-3551 cm<sup>-1</sup>, rocking band at ~ 837 cm<sup>-1</sup> and twisting band at ~732 cm<sup>-1</sup>. The vibrational frequencies of M-O and M-N bonds which appear at ~519 cm<sup>-1</sup> and ~ 470 cm<sup>-1</sup> respectively confirm the bonding between metal ions with the ligand through phenolic oxygen and azo nitrogen atoms[20]. The IR data suggest that the ligand is bonded with the metal ions through azo nitrogen and phenolic oxygen and carboxylic oxygen.



Graph-1 IR Spectrum of the ligand

Table-2 IR data of the ligand and complexes

Compound	$\nu(\text{C-O}) \text{ cm}^{-1}$	$\nu(\text{N=N}) \text{ cm}^{-1}$	$\nu(\text{COO}^+)_{\text{sym}} \text{ cm}^{-1}$	$\nu(\text{COO}^+)_{\text{asym}} \text{ cm}^{-1}$	$\nu(\text{M-O}) \text{ cm}^{-1}$	$\nu(\text{M-N}) \text{ cm}^{-1}$
1	1438	1588	1270	1625	-	-
2	1403	1470	1307	1599	519	470
3	1405	1472	1304	1598	518	474
4	1406	1476	1306	1597	517	472
5	1402	1475	1306	1599	518	470



Graph-2 IR Spectrum of the Co(II) complex

**1.LH<sub>2</sub>, 2.[Co<sub>4</sub>LCl<sub>4</sub>(H<sub>2</sub>O)<sub>12</sub>], 3.[Ni<sub>4</sub>LCl<sub>4</sub>(H<sub>2</sub>O)<sub>12</sub>], 4.[Cu<sub>4</sub>LCl<sub>4</sub>(H<sub>2</sub>O)<sub>12</sub>], [Zn<sub>4</sub>LCl<sub>4</sub>(H<sub>2</sub>O)<sub>4</sub>]**

**Electronic spectra and magnetic measurement**

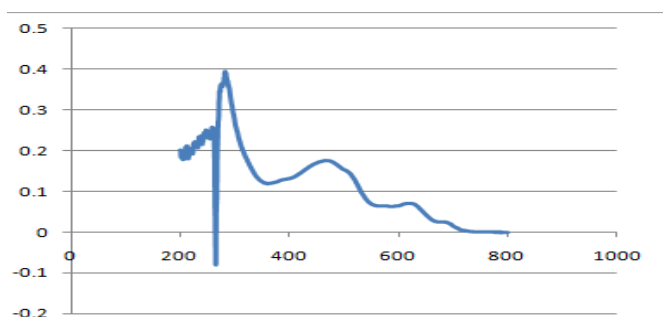
The electronic spectral and magnetic moment measurement data (Table-3) are used to confirm the geometry of the complexes as synthesis of single crystals of the complexes has been failed. The electronic spectrum of Co(II) complex(1) exhibits four bands at 10500, 16200 and 17450 cm<sup>-1</sup> assignable to <sup>4</sup>T<sub>1g</sub>(F) → <sup>4</sup>T<sub>2g</sub>(F) (ν<sub>1</sub>), <sup>4</sup>T<sub>1g</sub>(F) → <sup>4</sup>A<sub>2g</sub>(F) (ν<sub>2</sub>), <sup>4</sup>T<sub>1g</sub>(F) → <sup>4</sup>T<sub>2g</sub>(P) (ν<sub>3</sub>) transitions which are characteristic of octahedral geometry [21]. The fourth band is a CT band and the electronic parameters such as Dq, B, β, ν<sub>2</sub>/ν<sub>1</sub> and % σ are calculated by using following equations and given in the table-

$$Dq = \nu_2 - \nu_1/10$$

$$B = \nu_2 + \nu_3 - 3 \nu_1/15$$

$$\beta_{35} = B/971$$

$$\% \text{ of } \beta_{35} = (1 - \beta_{35}) \times 100$$



Graph-3 Electronic Spectrum of Ni(II) complex

Similarly, the Ni(II) complex(2) (Graph-3) also exhibits three d-d transition three bands at 12100, 15150, 23500 cm<sup>-1</sup> corresponding to <sup>3</sup>A<sub>2g</sub>(F) → <sup>3</sup>T<sub>2g</sub>(F), <sup>3</sup>A<sub>2g</sub>(F) → <sup>3</sup>T<sub>1g</sub>(F), <sup>3</sup>A<sub>2g</sub>(F) → <sup>3</sup>T<sub>1g</sub>(P) transitions, these suggest octahedral geometry for the Ni(II) complex [22]. The fourth band is a CT band and parameters like Dq, B, β, ν<sub>2</sub>/ν<sub>1</sub> and % β<sub>35</sub> are calculated by using following equations

$$Dq = \nu_1/10$$

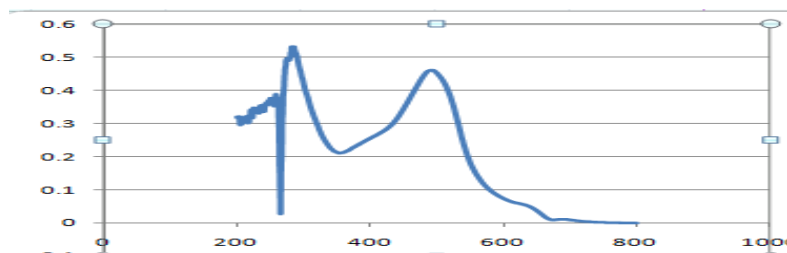
$$B = \nu_2 + \nu_3 - 3 \nu_1/15$$

$$\beta_{35} = B/1041$$

$$\% \text{ of } \beta_{35} = (1 - \beta_{35}) \times 100$$

The Racah parameter (B) of the Co(II) and Ni(II) complexes are found to be less than the free ion values and Nephelauxetic (β<sub>35</sub>) parameter for both the complexes is less than one. All these observations suggest that the metal ligand bonds in the complexes are covalent in nature.

The spectrum of Cu(II) complex(Graph-4) shows a CT bands at  $32467\text{ cm}^{-1}$  and  $19607\text{ cm}^{-1}$  and one d-d transitions band at  $15384\text{ cm}^{-1}$  which may be assigned to  ${}^2E_g \rightarrow {}^2T_{2g}$  transition supporting a distorted octahedral configuration for the complex[23, 24].



Graph-4 Electronic Spectrum of Cu(II) complex

The magnetic moment of the Co(II), Ni(II) and Cu(II) complexes are found to be 1.97 B.M. ,1.59 B.M. and 0.99 B.M. respectively in place for the theoretical value of 3.87 for Co(II), 2.97 Ni(II) and 1.87 for Cu(II) complex. The sub-normal magnetic moment values is due to anti-ferromagnetism which may arise due to mutual pairing of electron spins through super-exchange in a dimeric structure(M-O-M) or metal-metal interactions[25]. The Zn(II) complex is found to be diamagnetic, hence tetrahedral geometry is suggested from the analytical and magnetic data.

Table-3 Electronic parameters and Magnetic moment data

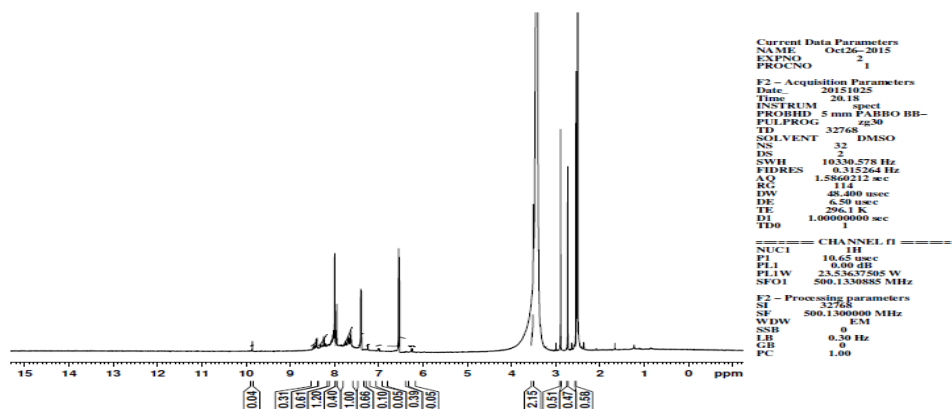
compound	$\lambda_{\text{max}}$ ( $\text{cm}^{-1}$ )	Transitions	B $\text{cm}^{-1}$	$\beta_{35}$ $\text{cm}^{-1}$	$\nu_2/\nu_1$	$\beta^0$	Geometry	$\mu_{\text{eff}}$ (BM)
1	8500 16200 20450 31250	${}^4T_{1g}(\text{F}) \rightarrow {}^4T_{2g}(\text{F})$ ${}^4T_{1g}(\text{F}) \rightarrow {}^4A_{2g}(\text{F})$ ${}^4T_{1g}(\text{F}) \rightarrow {}^4T_{2g}(\text{P})$ CT band	750	.772	1.90	22.8	octahedral	1.97
2	12820 16129 22727 32786	${}^3A_{2g}(\text{F}) \rightarrow {}^3T_{2g}(\text{F})$ ${}^3A_{2g}(\text{F}) \rightarrow {}^3T_{1g}(\text{F})$ ${}^3A_{2g}(\text{F}) \rightarrow {}^3T_{1g}(\text{P})$ CT band	25.7	.024	1.25	97.6	octahedral	1.59
3	15384 19607 32467	${}^2E_g \rightarrow {}^2T_{2g}$ CT band CT band	-	-	-	-	Distorted octahedral	0.99

### 1.[ $\text{Co}_4\text{LCl}_4(\text{H}_2\text{O})_{12}$ ], 2.[ $\text{Ni}_4\text{LCl}_4(\text{H}_2\text{O})_{12}$ ], 3.[ $\text{Cu}_4\text{LCl}_4(\text{H}_2\text{O})_{12}$ ]

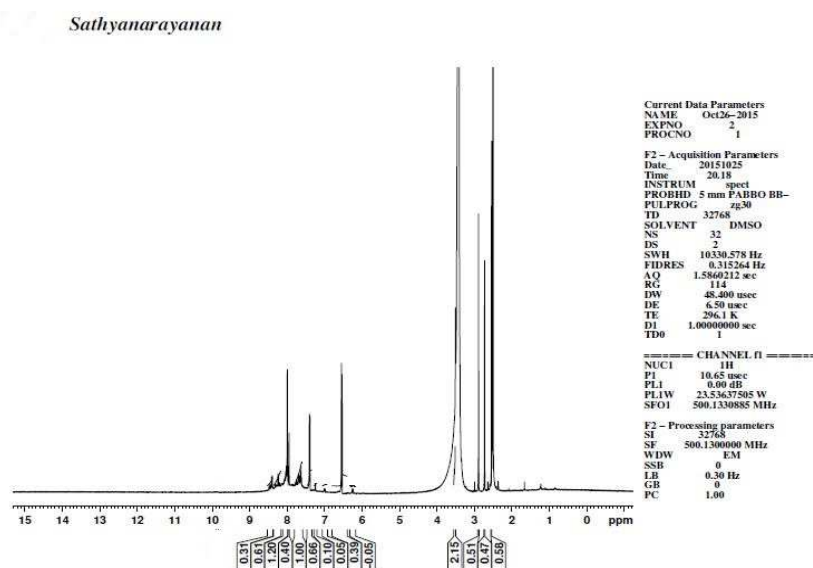
#### ${}^1\text{H}$ NMR spectra

The spectra of the ligand(Graph-5) and Zn(II)(Graph-6) complex were recorded in  $\text{DMSO-d}_6$  solvent. The  ${}^1\text{H}$  NMR spectrum of the ligand shows multiplet at  $\delta$  6.24-8.49 ppm which may be assigned to aromatic protons. The peak at  $\delta$  9.86 ppm corresponds to phenolic -OH group or -COOH as a single peak is observed due to exchange of protons between neighbouring -OH and -COOH groups[26].

S-I.....Sathyanarayanan



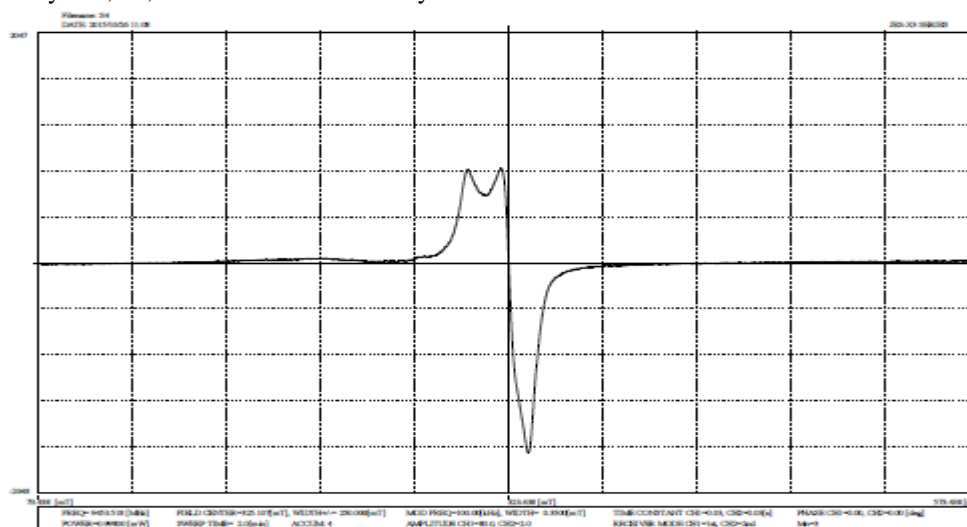
Graph-5  ${}^1\text{H}$  NMR spectra of the ligand

Graph-6  $^1\text{H}$  NMR spectrum of the Zn(II) complex

The spectrum of Zn(II) complex( was compared with the azo dye ligand and it is observed that the peak due to  $-\text{OH}$  and  $-\text{COOH}$  groups found in the ligand was absent in the complex. This indicates deprotonation of  $-\text{OH}$  and  $-\text{COOH}$  groups and formation of metal-O bond[27] in accordance with the data revealed by IR.

#### ESR spectrum

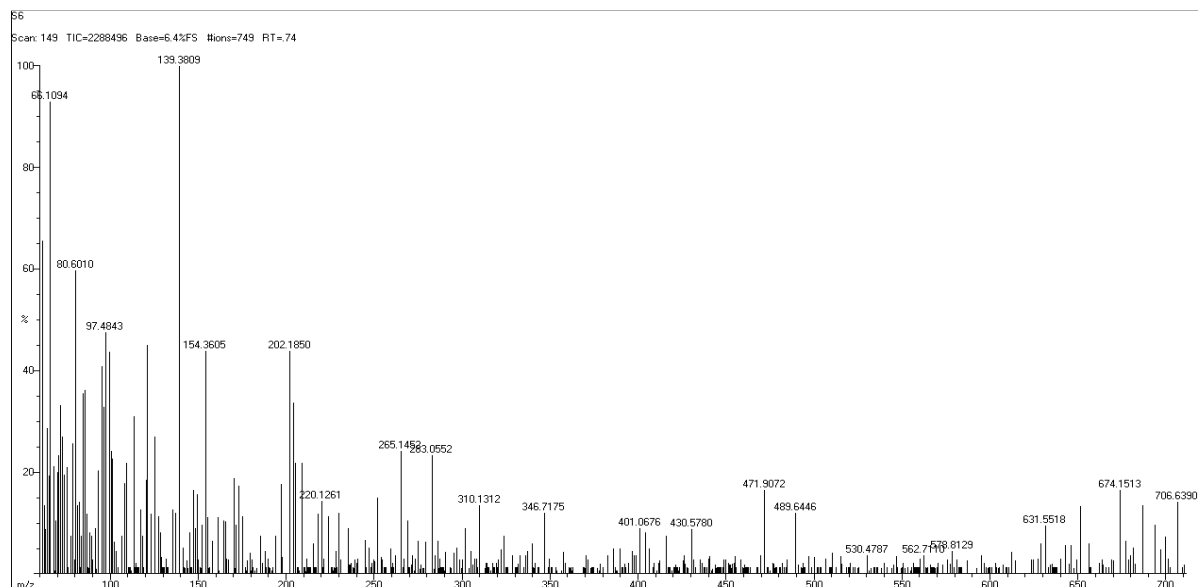
The esr spectrum(Graph-7) of the powdered Cu(II) complex is recorded at X band at room temperature to ascertain the stereochemistry of the Cu(II) complex. The copper complex exhibits the  $g_{\parallel}$  and  $g_{\perp}$  value as 2.11 and 2.03 respectively and  $g_{\parallel} > g_{\perp} > 2.0023$  these values indicate that the ground state is  $d_{x^2-y^2}$  and Cu(II) complex has an tetragonal geometry[28], the electronic spectral data of Cu(II) also supports this findings. The axial symmetric parameter (G) is calculated as 3.6 by using the equation  $G = \frac{g_{\parallel} - 2}{g_{\perp} - 2}$  which indicates considerable exchange interaction in the solid complexes since the value is less than four[29]. The  $g_{av}$  value is found to be 2.05 by following the equation  $g_{av} = \frac{1}{3}(g_{\parallel} + 2g_{\perp})$  and the spin-orbit coupling constant ( $\lambda$ ) is determined by using the equation  $g_{av} = 2(1 - \frac{2\lambda}{10dq})$ . The value of  $\lambda$  for the Cu(II) complex is found to be  $-384.6$  which is less than the free ion value( $-830 \text{ cm}^{-1}$ ). This lowering of  $\lambda$  value from the free ion value indicates overlapping of the orbitals of metal and ligand[30]. As the value of  $g_{\parallel}$  is  $< 2.3$ , the bonding between metal ligand is purely covalent as suggested by Kivelson and Neiman[31].The Cu(II) complex is suggested to be a distorted octahedral complex based on its analytical, IR, electronic and ESR study



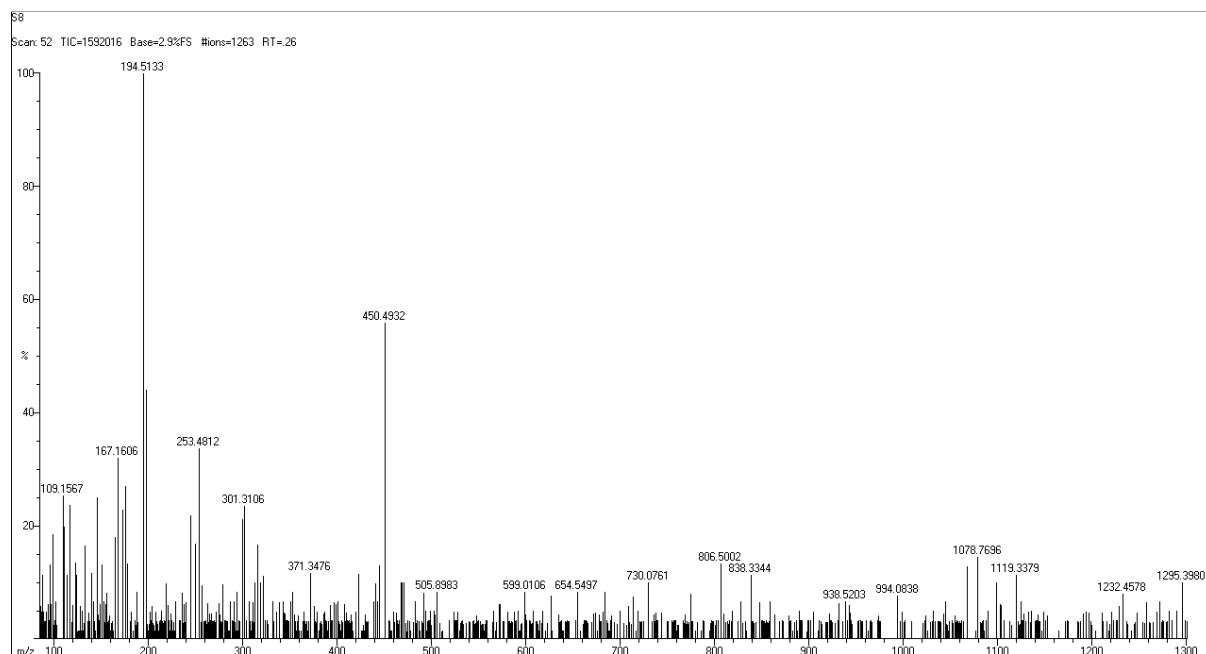
Graph-7 ESR spectrum of the Cu(II) complex

### MASS spectra

The mass spectra of the ligand(Graph-8) and its Ni(II) complex(Graph-9) are recorded at room temperature and spectra are used to compare their stoichiometric composition. The ligand( $C_{26}H_{18}N_4O_{14}S_3$  with molecular mass 706.63) shows a molecular ion peak at  $m/z$  706.639 amu which indicates the molecular mass of the ligand is in good agreement with the calculated molecular mass of the ligand from its proposed structure and other peaks appeared at  $m/z$  674.15, 631.55, 489.64, 471.92, 430.57 etc in the spectrum can be attributed to the fragmentation of the ligand molecule. A peak is observed at  $m/z$  129.39 amu in the spectrum of Ni(II) complex which corresponds to the stoichiometric composition of  $[Ni_4LCl_4(H_2O)_{12}]$ , other peaks are also observed at different position due to rupture of bonds of the Ni(ii) complex.



Graph-8 Mass spectra of the ligand

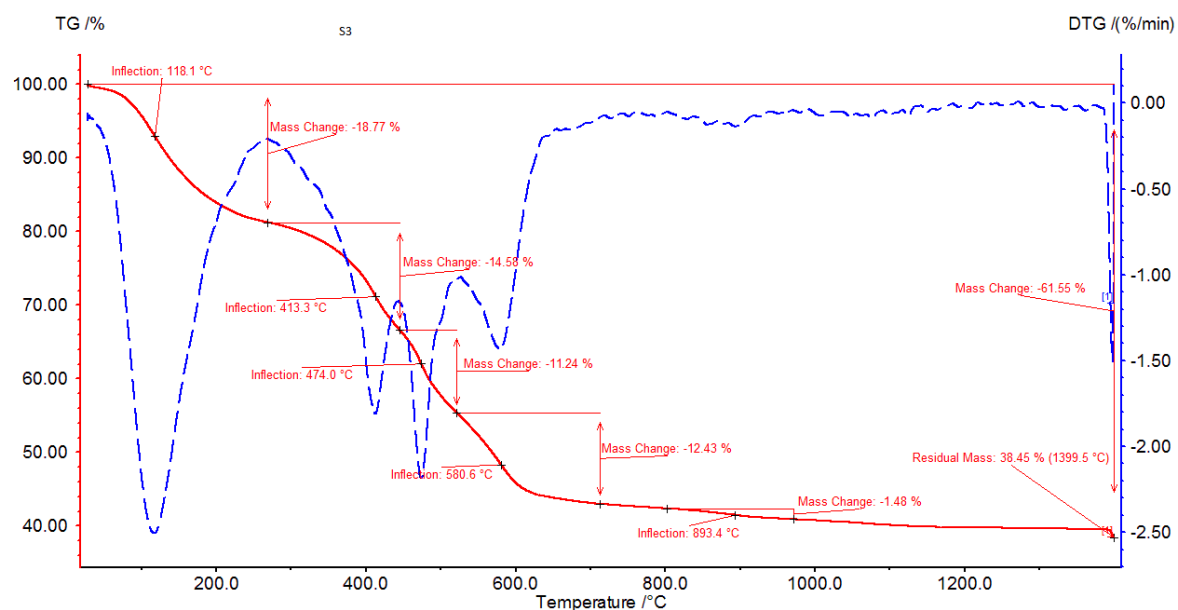


Graph-9 Mass spectrum of the Co(II) complex

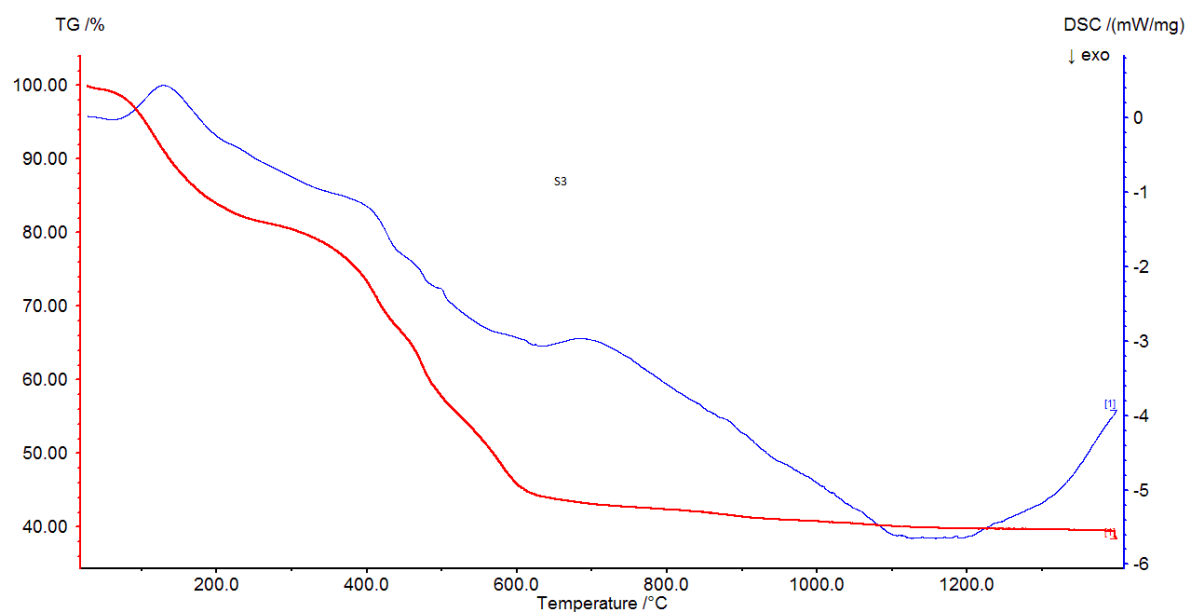
### Thermal study

The thermo gravimetric study of the Ni(II)(Graph-10,11) complex as a representative member of the investigating complexes is carried out by the simultaneous TG,DTG and DSC techniques in the atmosphere of nitrogen at a rate of  $10\text{ }^\circ\text{C}$  per minute from the ambient temperature to  $1400\text{ }^\circ\text{C}$ . The TG /DTG curves show that the complex suffers mass loss in a number of stages. The complex loses a mass of 18.77 % at  $118.77\text{ }^\circ\text{C}$  in the first stage, with an endothermic peak at 129.6 in the DSC curve. In the second stage, it suffers a mass of 14.58 % at  $413\text{ }^\circ\text{C}$  with a

endothermic peak at 402. The complex compound loses a mass of 11.24% in the third stage at 474°C with an endothermic peak 495.6. In the subsequent stages it loses a mass of 12.43% and 1.48% at 580.6°C and 893.4°C therefore, it is supported by an endothermic peak at 631.9. The complex suffers a total mass loss of 61.56% and its residual mass is 38.45% up to 1400°C. This study indicates the thermal stability of the complex.



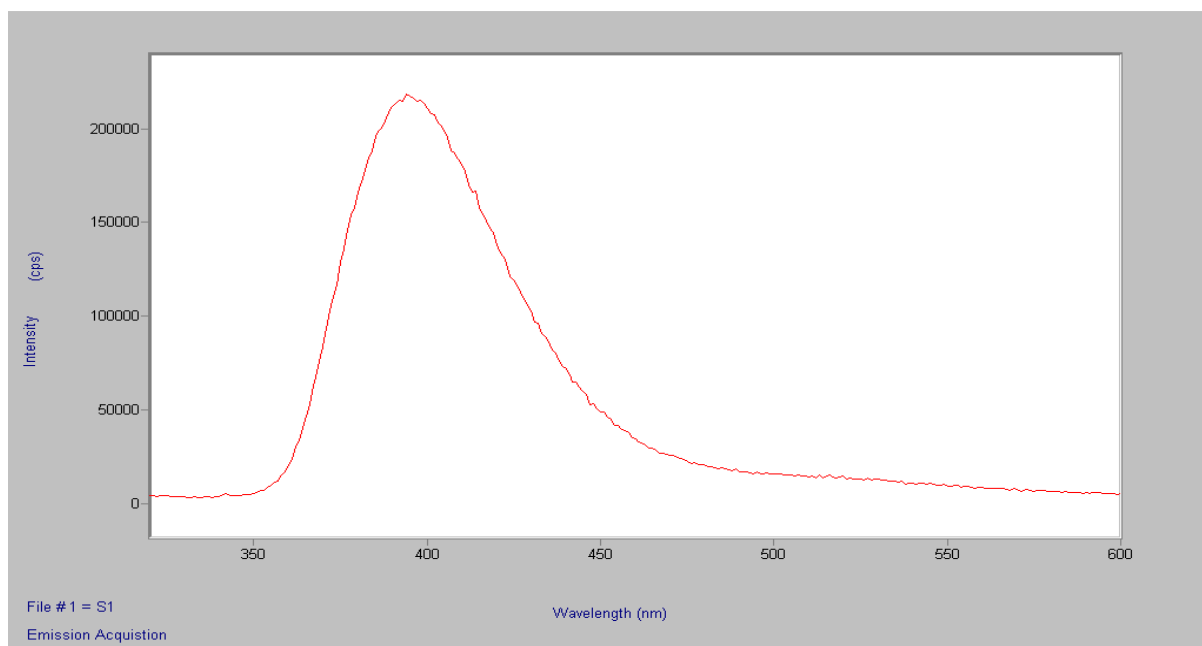
Graph-10 TG/ DTG Graph of the Ni(II) complex



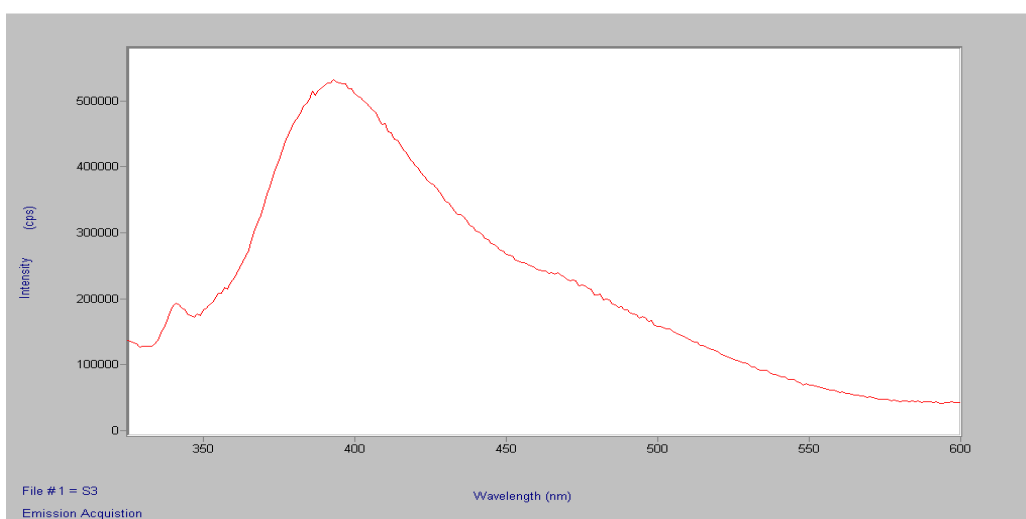
Graph-11 DSC Graph of the Ni(II) complex

#### Fluorescence study

The photoluminescence properties of the ligand and its complex are studied at room temperature in order to find their potential applications. The emission spectrum (Graph-12) of the ligand shows a maximum at 390 nm and the Ni(II) complex (Graph-13) shows a maximum at 400 nm. The emission intensity of the complex is found to be higher than the ligand and the enhanced intensity may be attributed to coordination thus increasing the rigidity thereby reducing energy loss by thermal vibration. The increase in intensity of the metal complex may also be due to metal to ligand charge transfer [32]. The fluorescent study suggests that both the ligand and its complexes can be used as making photoconductive materials [33].



Graph-12 Emission spectra of the ligand

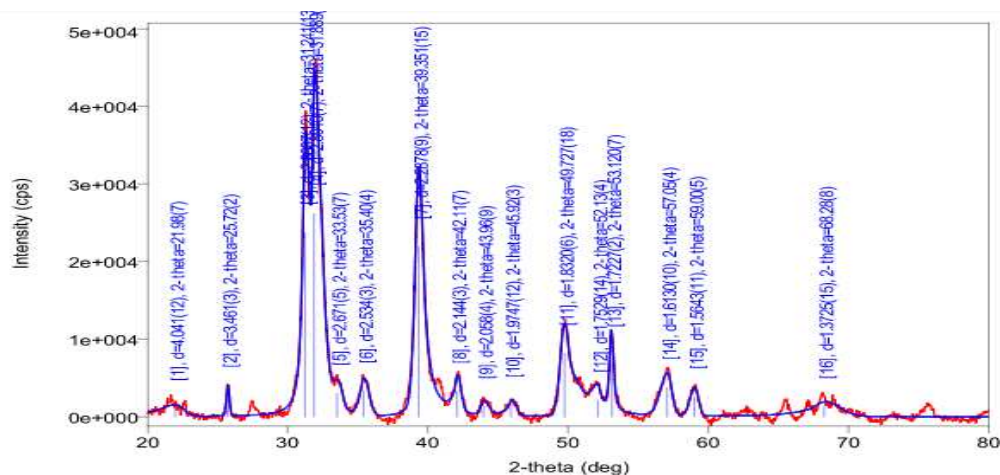


Graph-13 Emission spectra of Ni(II) complex

#### XRD study

The XRD (powder pattern) study of the Cu(II) complex (Graph-14) Table-4 and is made to determine its crystal system and particle size. The X-ray powder diffraction diagram is collected from the X'Pert diffractometer and the recording conditions are 40 kv and 40 mA for CuK $\alpha$  with  $\lambda = 1.542 \text{ \AA}$  between  $20^\circ$  to  $80^\circ$  with a step size of  $0.0089^\circ$ .

The XRD powder pattern is processed in X'pert high score software package. The search matching procedure is adopted for the PXRDPattern package and revealed a match with a copper compound corresponding JCPDS powder diffraction file with PDF No 700660. The pattern can be indexed to be a ANORTHIC crystal system with  $a=8.188$ ,  $b=8.778$ ,  $c=7.219$ ,  $\alpha=93^\circ$ ,  $\beta=96.50$ , lattice-primitive and space group is  $p_1(2)$ .



Graph-14 XRD(Powder pattern) of the complex

Table-4 XRD data of the Cu(II) complex at room temperature

Sl no	2 $\theta$ (degree)	D	FWHW(degree)	Intensity(cps degree)
1	21.98(7)	4.041(12)	2.1(3)	3169(1003)
2	25.72(2)	3.461(3)	0.249(18)	731(68)
3	31.2419(13)	2.8607(12)	0.63(3)	18557(787)
4	31.889(8)	2.8040(7)	0.709(13)	21446(860)
5	33.53(7)	2.671(5)	0.93(17)	3774(832)
6	35.40(4)	2.534(3)	0.74(6)	3193(244)
7	39.351(15)	2.2878(9)	0.716(7)	22442(310)
8	42.11(7)	2.144(3)	0.54(9)	2469(245)
9	43.96(9)	2.058(4)	0.58(8)	768(141)
10	45.92(3)	1.9747(12)	0.60(9)	1298(130)
11	49.727(18)	1.8320(6)	0.88(3)	11933(287)
12	52.13(4)	1.7529(14)	0.76(8)	2253(256)
13	53.12(7)	1.7227(2)	0.276(14)	2920(156)
14	57.05(4)	1.6130(10)	0.92(3)	3663(143)
15	59(5)	1.5643(11)	0.68(4)	1850(94)
16	68.28(8)	1.3725(15)	2.3(3)	4243(368)

### Surface morphology study

The surface morphology study of the Zn(II) complex of the ligand as a representative of all complexes is undertaken to evaluate its morphology and particle size. It is seen from the SEM image of the complex that the size of the particles is 10  $\mu\text{m}$  with the formation single phase morphology.

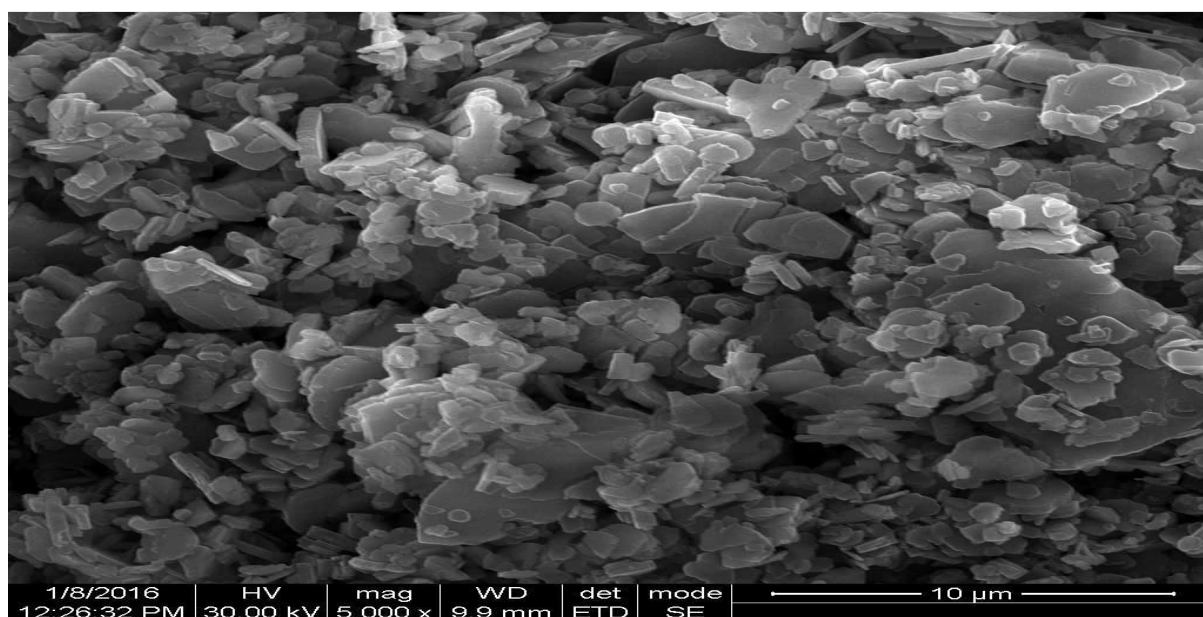


Image no-1 SEM image of Zn(II) complex

### Computational study

The structures of the ligand and all metal complexes are optimised at B3LYP[34] level of theory using 6-311++G(d,p) basis set. Gauss view 4.1[35] and chemcraft[36] are used to draw the structures. 6-311++G(d,p) is a large basis set which include diffused and polarised wave functions to take in to account the characteristics associated with ionic species having heavy atoms like N. The harmonic frequency calculation was also carried out at the same level of theory to ensure that the structures are true minima. Optimised was performed without any symmetry constraint using the default convergence criteria provided in the software

The reactive descriptors such as chemical potential, hardness and electrophilicity along with geometrical parameters of the ligand and its metal complexes are computed in order to know the reactivity and structure of the compounds theoretically.

Conceptual DFT defines chemical potential  $\mu$  as the first derivative of energy with respect to number of electrons

$$\mu = (dE/dN)_{V(r)}$$

where E= energy, N= number of electrons of the system at constant external pressure V(r).

chemical hardness  $\eta$  as the half of the second derivative of energy with respect to number of electrons, so chemical hardness will be the first derivative of energy with respect to number of electrons

$$\eta = 1/2(d^2E/dN^2)_{V(r)}$$

But chemical potential( $\mu$ ) and chemical hardness( $\eta$ ) are also calculated in most cases in terms ionisation potential(IP) and electron affinity(EA) and therefore

$$\mu = -(IP+EA)/2 \text{ and } \eta = (IP-EA)/2$$

According Koopman's theorem, IP and EA are related to energies of the Highest occupied molecular orbital( $E_{HOMO}$ ) and Lowest occupied molecular orbital( $E_{LUMO}$ ) in this way,  $IP = -E_{HOMO}$  and  $EA = E_{LUMO}$

$$\eta = E_{HOMO} - E_{LUMO}/2 \text{ and } \mu = E_{HOMO} + E_{LUMO}/2$$

and Parr and coworkers proposed electrophilicity[37] as a measure of electrophilic power of a compound the electrophilicity can be represented as

$$\omega = \mu^2/2\eta$$

The dipole moment( $\mu$ ) and global reactive descriptors of the ligand and its metal complexes are calculated from their HOMO and LUMO values and summarised (Table-4). The data shows that the electrophilicity value of the complexes are more than the free ligand therefore the complexes are more reactive than the ligand. According to minimum electrophilicity principle, lesser is the electrophilicity of a compound, more will be its stability so the order of reactivity of the complexes are  $[Cu_4LCl_4(H_2O)_{12}] > [Zn_4LCl_4(H_2O)_4] > Ni_4LCl_4(H_2O)_{12} > [Co_4LCl_4(H_2O)_{12}]$

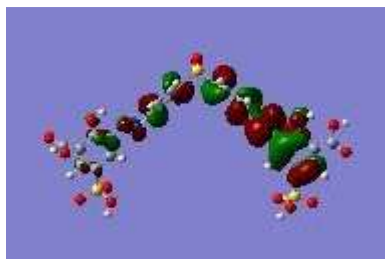


Fig-3 (HOMO of Ligand)

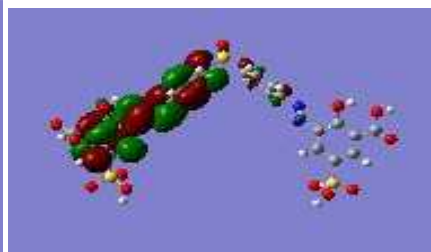


Fig-4 (LUMO of Ligand)

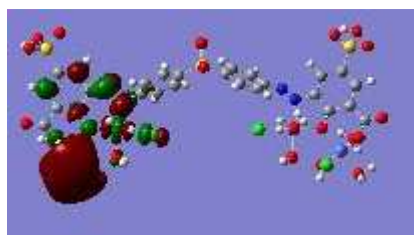


Fig-5 (HOMO of Co(II) complex)

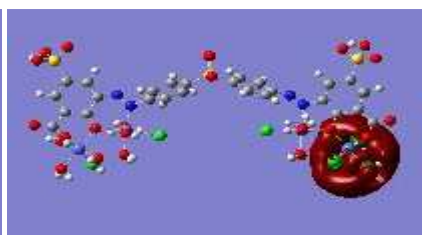


Fig- 6(LUMO of Co(II) complex)

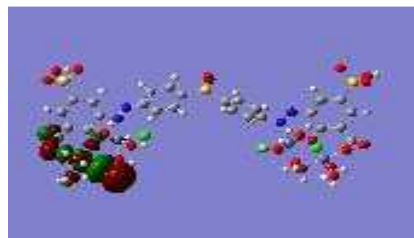


Fig-7 (HOMO of Ni(II) complex)

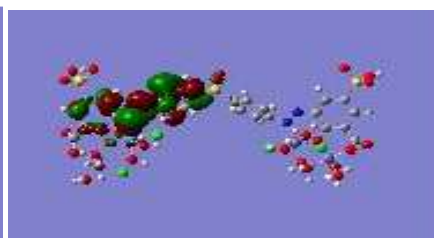


Fig- 8(LUMO of Ni(II) complex)

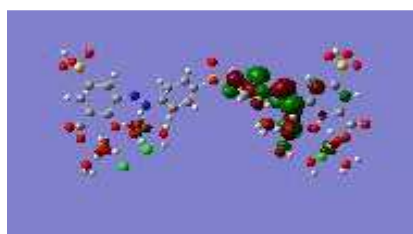


Fig-9 (HOMO of Cu(II) complex)

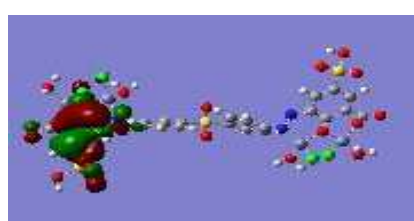


Fig- 10(HOMO of Zn(II) complex)

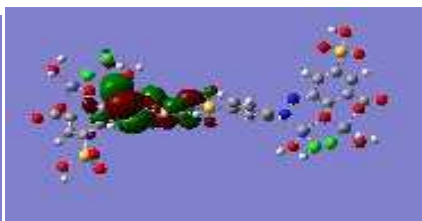


Fig-11 (LUMO of Zn(II) complex)

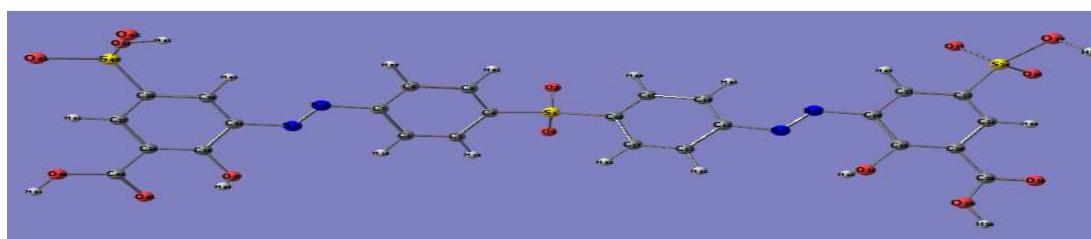


Fig-12 Optimised geometry of the ligand

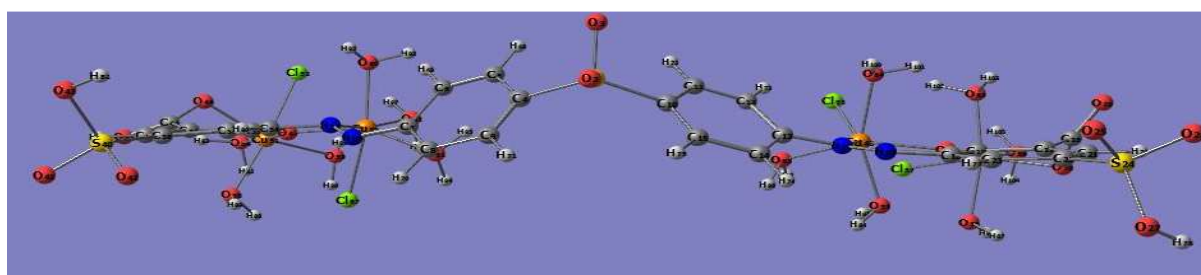


Fig-13 Optimised geometry of Cu(II) complex

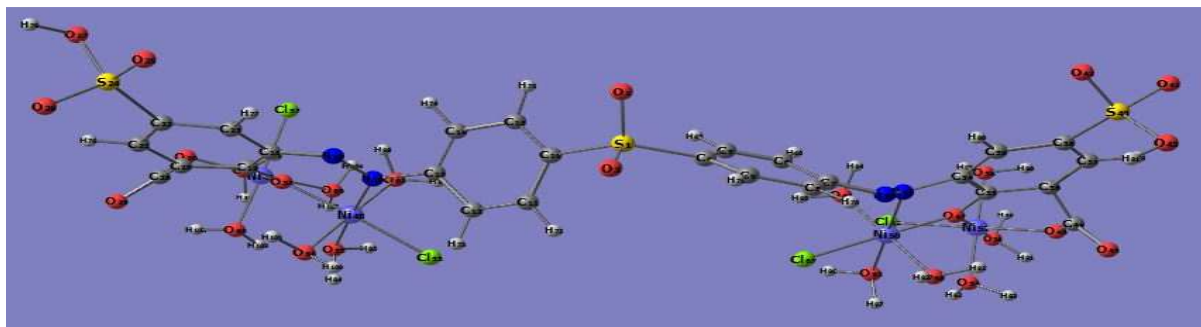


Fig-14 Optimised geometry of Ni(II) complex

Table-4 Global Reactive indices and dipole moment of the investigated compounds

compound	HOMO	LUMO	n(eV)	$\mu$ (eV)	$\omega$	$\mu$ (D)
LH <sub>2</sub>	-0.35865	0.01262	0.1856	-0.1730	0.0806	7.7752
[Co <sub>4</sub> LCl <sub>4</sub> (H <sub>2</sub> O) <sub>12</sub> ]	-0.10461	-0.04461	0.03	-0.0746	0.0927	46.8586
[Ni <sub>4</sub> LCl <sub>4</sub> (H <sub>2</sub> O) <sub>12</sub> ]	-0.28802	-0.06599	0.111	-0.1767	0.140	27.1316
[Cu <sub>4</sub> LCl <sub>4</sub> (H <sub>2</sub> O) <sub>12</sub> ]	-0.21887	-0.09067	0.064	-0.1547	0.187	26.4345
[Zn <sub>4</sub> LCl <sub>4</sub> (H <sub>2</sub> O) <sub>4</sub> ]	-0.39813	-0.06604	0.166	-0.2320	0.162	6.3383

Table-5 Selected bond length and bond angle

compound	Bond length(Å)				Bond angle(°)		
	N(16)-N(17)	N(17)-C(18)	O(31)-C(29)	N(16)-M(48)	N(16)-M(48)-O(31)	N(16)-M(48)-O(55)	N(16)-M(48)-Cl(53)
1	1.225	1.454	1.364	-	-	-	-
2	1.246	1.417	1.282	1.952	94.513	88.565	92.774
3	1.243	1.438	1.281	1.976	102.754	92.239	94.839
4	1.254	1.403	1.314	2.034	95.708	110.284	98.964

#### 1.LH<sub>2</sub>, 2.[Ni<sub>4</sub>LCl<sub>4</sub>(H<sub>2</sub>O)<sub>12</sub>], 3.[Cu<sub>4</sub>LCl<sub>4</sub>(H<sub>2</sub>O)<sub>12</sub>], 4. [Zn<sub>4</sub>LCl<sub>4</sub>(H<sub>2</sub>O)<sub>4</sub>]

##### Nonlinear optical properties

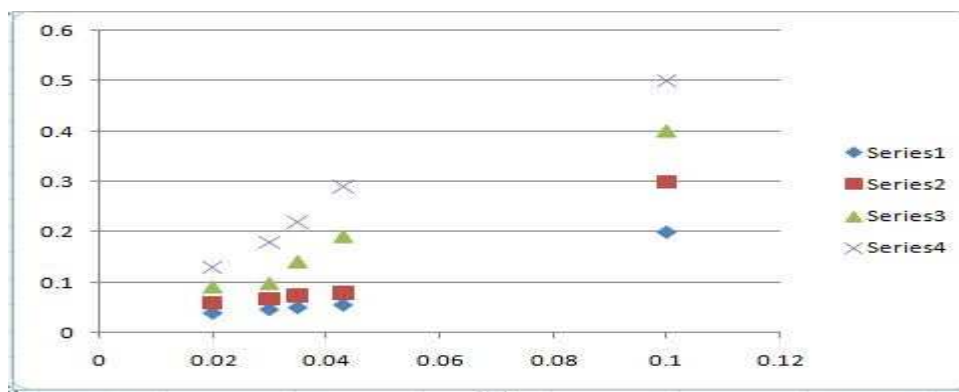
The electronic properties of chemical compounds are related to their non-linear optical activities. Easy electron transition between molecular orbitals is the basic requirement for good nonlinear optical materials. It is seen from the Table that all metal complexes except Zn(II) complex have higher dipole moment than the free ligand. The energy gap between the HOMO and LUMO of the ligand is found to be higher than the complexes. All these findings indicate that complexes have better nonlinear properties[38] than the free organic ligand. The Co(II) complex will be the good nonlinear optical material due to small energy gap

##### Biological activity study

##### DNA binding Test

##### Viscosity Measurement

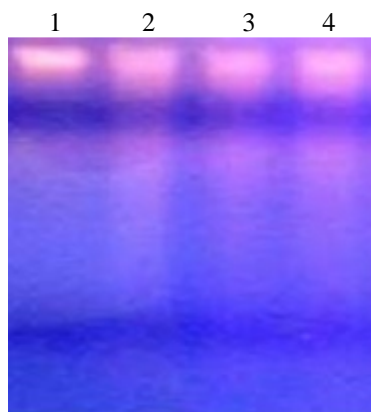
Viscosity measurement(Graph-15) of the DNA and test solutions consisting of DNA and metal complexes is made in order to confirm the interaction between compounds and DNA. The increase in viscosity of DNA occurs when the complexes intercalate between the base pairs due to extension in the helix[39]. The effects of all the synthesised complexes on the viscosity of DNA are shown in the graph-. The graph shows that viscosity of DNA increases with increase in the concentration of complexes and the order of increase of viscosity is [Cu<sub>4</sub>LCl<sub>4</sub>(H<sub>2</sub>O)<sub>12</sub>] > [Zn<sub>4</sub>LCl<sub>4</sub>(H<sub>2</sub>O)<sub>4</sub>] > [Co<sub>4</sub>LCl<sub>4</sub>(H<sub>2</sub>O)<sub>12</sub>] > [Ni<sub>4</sub>LCl<sub>4</sub>(H<sub>2</sub>O)<sub>12</sub>].



Graph-15 [Series-4-Cu(II) complex+DNA,3- Zn(II) complex, 2- Co(II) complex and 1- Ni(II) complex]

#### Gel electrophoresis

The interaction between complex and metal complexes is also studied by gel electrophoresis. The electrophoresis study shows that intensity of the DNA-complex bands are less than the DNA control and the intensity decreases in the order of  $[\text{Cu}_4\text{LCl}_4(\text{H}_2\text{O})_{12}] > [\text{Ni}_4\text{LCl}_4(\text{H}_2\text{O})_{12}] > [\text{Co}_4\text{LCl}_4(\text{H}_2\text{O})_{12}]$  (lane 2- Co(II) complex, lane 3 - Ni(II) complex, lane 4- Cu(II) complex and lane 1- DNA CONTROL). Due to the intercalation of the metal complexes in to the DNA base pairs, intensity decreases.



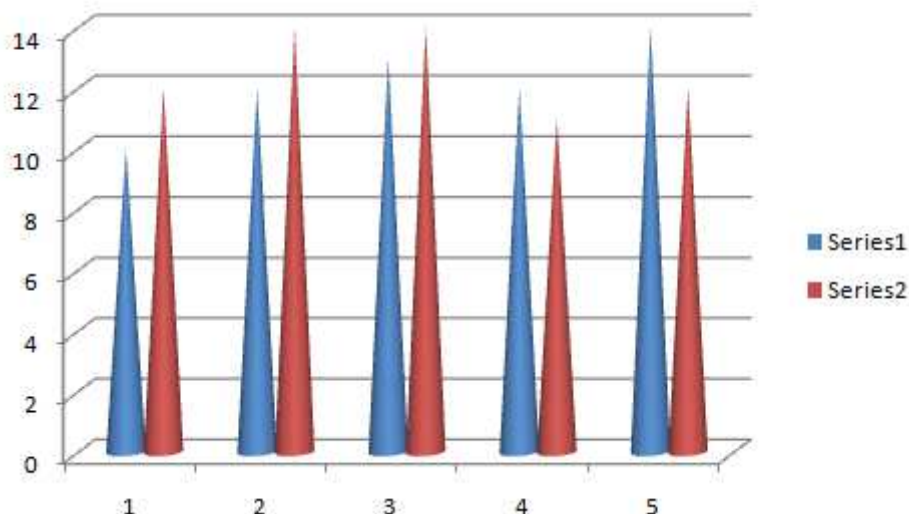
Graph-[From left 1-DNA CONTROL,2-Co(II),3- Ni(II) and 4-Cu(II)]

#### Antibacterial study

All the test compounds are screened (table-6) against the gram positive *S. aureus* and gram negative bacterial *E. coli*. The ligand and its complexes have moderate effect on the growth of the microorganism. The complexes have potent antibacterial properties than the ligand and the order of the activity is given in the graph. The enhanced antibacterial activities of the complexes can be explained by taking in to account chelation and overtone's concept. According to chelation theory, the polarity of the metal ions is reduced due to the overlapping of ligand orbitals with the metal ions [40]. The lipophilicity of the complexes is also enhanced due to delocalisation of the  $\pi$  electrons of the ligand over the entire chelate ring. The lipophilic substances can easily enter in to the microorganisms by penetrating through the cell membrane according to overtone's concept and inhibits the growth of microorganisms.

Table-6 Antibacterial Screening of the title compounds

compound	concentration	<i>E. coli</i>	<i>S. aureus</i>
1. $\text{LH}_2$	500 $\mu\text{g/ml}$	10	12
2. $[\text{Co}_4\text{LCl}_4(\text{H}_2\text{O})_{12}]$	500 $\mu\text{g/ml}$	12	14
3. $[\text{Ni}_4\text{LCl}_4(\text{H}_2\text{O})_{12}]$	500 $\mu\text{g/ml}$	13	14
4. $[\text{Cu}_4\text{LCl}_4(\text{H}_2\text{O})_{12}]$	500 $\mu\text{g/ml}$	14	16
5. $[\text{Zn}_4\text{LCl}_4(\text{H}_2\text{O})_4]$	500 $\mu\text{g/ml}$	14	12
6. Tetracycline	500 $\mu\text{g/ml}$	30	30



### CONCLUSION

The ligand acted as a hexa dentate ligand as it coordinated with the metal atoms through OON-NOO donor atoms. On the basis of analytical and spectral data and Computational study distorted octahedral geometry for the Co(II), Ni(II), Cu(II) and distorted tetrahedral geometry for Zn(II) was proposed. Thermal study of the metal complex indicates thermal stability of the complexes, the fluorescence studies reveals that both ligand and its metal complexes have fluorescent properties and can be used for making photo conducting materials. The ligand and its complexes are known to have antibacterial properties and DNA binding abilities as indicated from their biological studies.

### Acknowledgements

Author acknowledges UGC for financial support in the form of Minor Research Project and SAIF IIT CHENNAI for providing spectral data.

### REFERENCES

- [1] A T Peters, H S Freeman, Colour chemistry, the design and synthesis of organic dye and pigments, Elsevier App. Sci. Publications, **1991**
- [2] W T Gao; Z. Zheng, *Molecules*, **2002**,7,511
- [3] A M Khedr; R M Issa Gaber; H Erten, *Dyes pigments*,**2005**,67,117-126
- [4] E M Hodnett; W J Dunn; *J. Med. Chem.*, **1970** ,13, 768-770
- [5] S Cunha; S M Rodrigues; MT Bastos, *J. Mol. Struct.*,**2005**,752,694-702
- [6] X Li ; Y Wu; D Gu ; F Gan, *Dyes Pigm.*, **2010**, 92, 691-709
- [7] Y Gang; D.Gu; F. Gan, *Opt matter*,**2004**, 27,193-197
- [8]. C Anita; C D Sheela; P Dharamraj; S Sumathi, *Spectrochimica Acta part A: Molecular and Bimolecular Spectroscopy*,**2012**,96,493-500
- [9] AC Tella; J A Obaleye, *E. Journal Of Chemistry*,**2009**, 6(S1),S311-S323
- [10] F Frisch, G Trucks, H Schlegel, G Scuseria, M Robb, J Cheeseman, jr, J Montgomery, T Ureven, K Kudin, J Burant, Gaussian 03 Rev B. O3,Gaussian Inc, Pittsburg, PA,2003
- [11] A D Beckel, *J.Chem. Phys.*, **1993**,98,564
- [12] D Sobolova; M Koz urkova; T Plichta; Ondrusova; Z Simkovic; M H Paulikova, A. Valent, *International Journal of Biological Macromolecules*,**2011**,48,319-325
- [13] L H Abdel-Rahman.; R. M. El-Khatib,.; L.A E.Nassr,.; A.M.Abu-Dief,.; F. El-Din Lashin, *Spectrochimica Acta PartA; Molecular Biomolecular Spectroscopy*, **2013**, 111,266-276
- [14] R S.Brant,; E R Miller, *J. Bacteriol*, **1939**,38(5),525
- [15] W J Geary, *Coord. Chem. Rev.*, **1971**,7, 81.
- [16] A Saxena; J P Topndon, *Polyhedron*, **1984**,3,681
- [17] S D Robinson; M F Uttley, *J. Chem. Soc.* **1973**,**1912**
- [18] R B King, *Inorganic Chemistry*,**1961**, 5, 300
- [19] V Stefov; V M Petrusevski; V M Soptrajanov, *B. J. Mol. Structure*,**1993**,97,293
- [20] K Nakamoto, *Infrared and Raman Spectra of Inorganic and Coordination compounds*, Wiley and sons,**2009**

- 
- [21] A B P Lever, *Coord. Chem. Rev.*, **1968**, 3, 119
- [22] M Shakir; A K Mahammed; O S M Nasman, *Polyhedron*, **1996**, 15, 3487-3492
- [23] A B P Lever, E I Solomon, *Inorganic Electronic Structure and Spectroscopy*, Wiley and sons, **2014**
- [24] S Yamada, *Coord. Chem. Rev.*, **1966**, 1, 445
- [25] M K S Abou; H Faruk, *J. of Iran Chem. Soc.*, **2008**, 5, 122-134
- [26] D H W.illiams, I Fleming, *Spectroscopic methods in organic chemistry*, TataMcGraw Hill, **1994**
- [27] A E Ahmed; M A E Taha, *Spectrochimica Acta Part A: Molecular Bimolecular Spectroscopy*, **2011**, 56, 2775-2781
- [28] A F M Benial; V Ramakrishan; R Murugesan, *Spectrochimica Acta Part A: Molecular Bimolecular Spectroscopy*, **2000**, 79, 1803-1814
- [29] B J Hathaway; D E Billing, *Coord. Chem. Rev.* **1970**, 5, 143
- [30] R L Dutta, A Syamal, *Elements of Magnetochemistry*, East –West Press PVT LTD, **2010**
- [31] D Kivelson; R R Neiman, *J. Chem. Phys.*, **1961**, 35, 159.
- [32] E Badaruddin; Z Aiyub; Z Abdullah, *The Mal. J. Of Anal. Sc.*, **2008**, 12(8), 285-290
- [33] A Majumdar; G M Rosair; A Mallick; N Chattopadhy; S. Mitra, *Polyhedron*, **2006**, 25(8), 1753-1762
- [34] A D Becke, *J. Chem. Phys.*, **1993**, 98, 5648-5642
- [35] R Dennington, T Keith, J Milliam, *Gauss View Version 4.1*, **2007**
- [36] G A Zhurko; D A Zhurko, *Chemcraft*, **2005** (Freeware)
- [37] R J Parr; R J Pearson, *J. Am. Chem. Soc.*, **1983**, 7512, 105
- [38] S M Soliman; M A M Abu-Youssef.; J Albering, A. El-Faham, *J. Chem. Sci.* **2015**, 12 2137-2149
- [39] P R Hertzberg; P B Dervan, *J. Am. Chem. Soc.*, **1982**, 104, 313-315
- [40] A B P Lever, *Journal of Molecular Structure*, **1985**, 129, 180-181